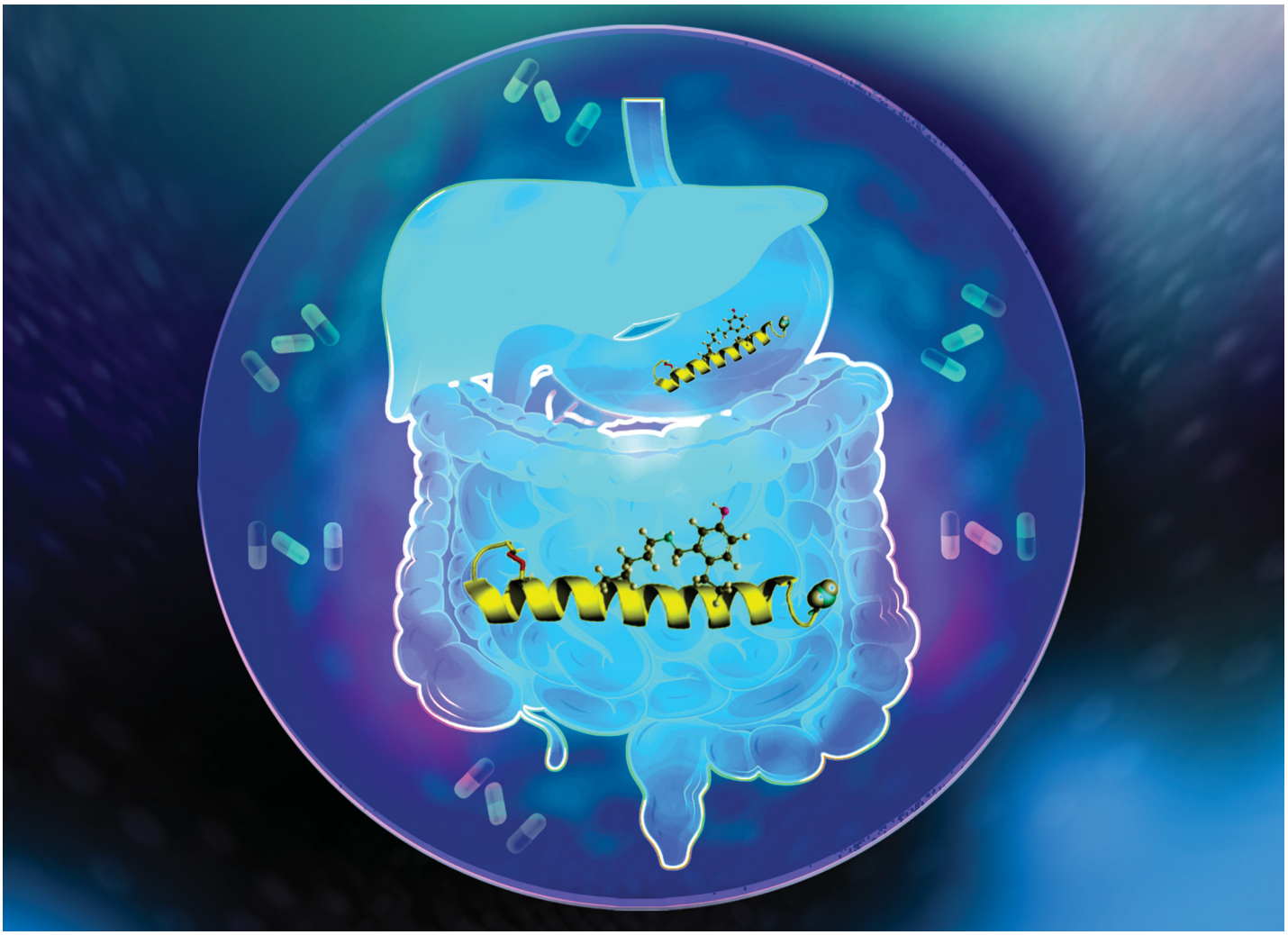

Showcasing research from Professor Norman Metanis' laboratory, Institute of Chemistry, The Hebrew University of Jerusalem, Jerusalem, Israel.

Enhancing the gastrointestinal stability of salmon calcitonin through peptide stapling

The stapling between Lys11 and Tyr22 of salmon calcitonin afforded a peptide with enhanced stability under gastrointestinal conditions, while maintaining activity. This is a starting point for the development of oral calcitonin for the treatment of postmenopausal osteoporosis and hypercalcemia.

As featured in:

See Hiba Ghareeb and Norman Metanis, *Chem. Commun.*, 2023, **59**, 6682.

ROYAL SOCIETY OF CHEMISTRY

rsc.li/chemcomm

Registered charity number: 207890

ChemComm

COMMUNICATION

View Article Online
View Journal | View Issue

Cite this: *Chem. Commun.*, 2023, 59, 6682

Received 8th March 2023,
Accepted 18th April 2023

DOI: 10.1039/d3cc01140b

rsc.li/chemcomm

Enhancing the gastrointestinal stability of salmon calcitonin through peptide stapling†

Hiba Ghareeb[a] and Norman Metanis *[abc]

Salmon calcitonin (sCT) is a polypeptide hormone available in the clinic. sCT is degraded in the gastrointestinal tract in minutes. In this work, a stapled analogue of salmon calcitonin, KaY-1(R24Q), was developed using the cooperative stapling between Lys and Tyr, with R24Q substitution. The analogue exhibited an improved stability in simulated gastric and intestinal fluid and retained the ability to activate the calcitonin receptor. This work will serve as a starting point for the development of an oral sCT drug.

Human calcitonin (hCT) is an endogenous hormone secreted by the parafollicular C cells of the thyroid gland, and plays a critical role in regulating calcium homeostasis and bone remodeling.[1] Its function is derived from its ability to inhibit bone resorption, and reduce osteoclast formation and attachment.[2] CT is found in various organisms including mammals and fish[3] and shares many structural features across species. This single-chain 32 amino acid polypeptide is characterized by an N-terminal disulfide bridge (between Cys1 and Cys7) and a proline amide at the C-terminus, while folding into a helical structure was found to be essential for receptor binding, especially through Gly28, Ser29, Gly30 and Thr31 (Fig. 1A and B).[4,5] The most widely used variant in the clinic is salmon calcitonin (sCT), since it has the highest affinity for the human calcitonin receptor (hCTR), and also the highest potency,[6] while hCT is known to form fibers.[7] Hence, sCT has been used for more than 40 years to treat postmenopausal osteoporosis, Paget's disease and hypercalcemia.[3] In addition, calcitonin reduces the risk of vertebral fracture recurrence and provides pain relief for acute back pain caused by vertebral fractures,[8] and is commercially available as an injection and nasal spray. The intra-muscular and subcutaneous injections are available as parenteral calcitonin dosage forms, which are associated with gastrointestinal (GI) disturbances and injection site reactions.[9,10] Intranasal administration *via* a nasal spray has many advantages over the parenteral form, such as convenience and being less invasive for patient, and fewer GI side effects. However, the nasal spray has lower bioavailability and slower absorption compared to the parenteral.[11]

Enhancing the stability of therapeutic peptides such as sCT in the GI tract will improve their therapeutic applications. Oral administration is the most convenient route for drug administration, due to its cost effectiveness, ease of ingestion, painlessness, and high patient compliance. However, peptides are vulnerable to enzymatic degradation in the GI tract, lowering

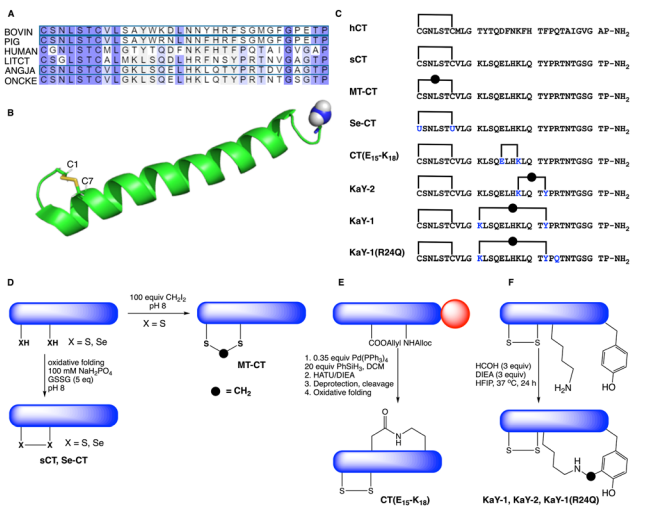

Fig. 1 The design and synthesis of CT variants. (**A**) Amino acid sequence of CT from different species sharing many structural features, all consisting of 32 residues, a highly helical structure, a disulfide bond between Cys1 and Cys7, and proline amide at the C-terminus. CALC_LITCT is American bullfrog, CALC_ANGJA is Japanese eel, and CALC1_ONCKE is salmon calcitonin. (**B**) The NMR structure of sCT (PDP entry 2GLG). (**C**) The amino acid sequences of hCT and sCT and their synthetic variants. (**D–F**) Peptides were obtained by Fmoc-SPPS with different cyclization strategies.

[a] *Institute of Chemistry, The Hebrew University of Jerusalem, Jerusalem 9190401, Israel. E-mail: metanis@mail.huji.ac.il*
[b] *Casali Center for Applied Chemistry, The Hebrew University of Jerusalem, Jerusalem 9190401, Israel*
[c] *The Center for Nanoscience and Nanotechnology, The Hebrew University of Jerusalem, Jerusalem 9190401, Israel*

† Electronic supplementary information (ESI) available. See DOI: https://doi.org/10.1039/d3cc01140b

their efficacy in patients to unacceptable levels.[12] One of the main obstacles to the development of oral CT is its degradation in the acidic environment of the gastric fluid and the proteases in the stomach and the intestine, among these enzymes pepsin, trypsin, chymotrypsin and elastase.[13] Although a number of oral sCT formulations have been developed to prevent protein degradation,[14] they failed phase III clinical studies, due to the insignificant effect in reducing the risk of vertebral and non-vertebral fractures.[15]

Many approaches can be used to stabilize peptides including helical peptide stapling, where crosslinking between side chains constrains the peptide's molecular flexibility, usually improving binding affinity, selectivity and stability.[16–19] Macrocyclic or helix stapled peptides are known to have higher resistance to protease degradation as well as enhanced potency and binding affinity.[20–22] Examples of crosslinking approaches include helix stabilization, such as lactam groups, disulfide mimics, hydrocarbon stapled peptides, and others.[23–26] In this work, we examined a number of modifications, including stapling the helical structure of sCT, to improve its stability while retaining its biological activity.

A number of CT analogues (Fig. 1C) were synthesized and their GI stability and the ability to bind to the calcitonin receptor were evaluated. We first started with the synthesis of sCT, followed by six different stapled analogues (MT-CT, Se-CT, CT(E_{15}–K_{18}), KaY-1, KaY-2 and KaY-1(R24Q)). All of these peptides were prepared by Fmoc-SPPS.[27] Peptides without disulfide mimics underwent oxidative folding with oxidized glutathione (GSSG), followed by purification and characterization by HPLC and ESI-MS (full details can be found in the ESI†).[28,29] We first set out to stabilize sCT's disulfide bridge between Cys1 and Cys7, which is inherently unstable to the reducing environments in biological systems. Many strategies have been employed to improve the metabolic stability of disulfide bonds, such as conversion to a methylene thioacetal bridge (MT),[30,31] or substitution of the disulfide bridge with a diselenide using selenocysteine (Sec, U),[32–34] thioether,[35,36] or other disulfide mimics.[37–39] We therefore designed and synthesized MT-CT, in which the methylene thioacetal (MT) crosslink is located between Cys1 and Cys7. The synthetic sCT (20 mg) was dissolved in a phosphate buffer containing guanidine hydrochloride, with tris(2-carboxyethyl)phosphine (TCEP) as a reducing agent (1.5 equiv.) to ensure that the Cys residues are in the reduced form. Next, an excess of diiodomethane (CH_2I_2) in DMSO was added and the reaction was stirred at 37 °C overnight (Fig. 1D).[30,31] The progress of the reaction was followed by HPLC and ESI-MS and the resulting MT-CT was isolated by Prep HPLC in 60% yield (12 mg). For Se-CT synthesis (with a Sec1 and Sec7), Sec residues were manually coupled *via* Fmoc-SPPS using DIC/OxymaPure and after cleavage and deprotection, the peptide was isolated in 25% yield (50 mg) (Fig. 1D).

Additionally, two methods were used to staple sCT in its iconic helical form: a lactam bridge between Lys and Glu, as well as a formaldehyde-based link between Tyr and Lys. In the more classical, lactam-based approach, the stapled helical peptide was stabilized through a side-chain to side-chain lactam crosslink between the ε-amino functional group of lysine (Lys, K) and the carboxyl moiety of glutamic acid (Glu, E) or aspartic acid (Asp, D). Such modifications have been found to improve both the potency and stability of peptides compared to their linear counterparts.[40–42] Accordingly, we synthesized a lactam crosslink between Glu15 and Lys18 (*i.e.*, CT(E_{15}–K_{18})), in which the lactam formation was performed on resin (Fig. 1E). Hence, orthogonal protecting groups (PGs) of Alloc/Allyl were used for Lys18 and Glu15, respectively. Both side chain PGs were deprotected on resin in a single step using a palladium catalyst,[43] followed by macrolactamization with HATU and DIEA. After peptide synthesis completion, deprotection and cleavage yielded the desired product, which was confirmed by MS, with a mass that was 18 Da lower than sCT. This synthesis provided 10 mg of CT(E_{15}–K_{18}) (33% yield) after prep HPLC purification (Fig. 1E).

More recently, a new type of stapling of linear peptides was reported by Chen and coworkers.[44,45] In this method, formaldehyde forms an imine with the ε-amino group of the Lys residue, followed by crosslinking to tyrosine (Tyr, Y) or arginine (Arg, R) residues in the polypeptide chain.[44,45] Using this approach, a reaction between sCT and formaldehyde, with DIEA in hexafluoroisopropanol (HFIP), resulting in crosslinks between the ε-amine of Lys and the phenol ring of Tyr will yield two different analogues, KaY-1 (Lys11-Tyr22 crosslink) and KaY-2 (Lys18-Tyr22 crosslink) (Fig. 1F). The treatment of 20 mg of sCT with 3 equiv. of HCOH and 3 equiv. of DIEA (Fig. 1F and Fig. S9, ESI†) gave two main stapled peptides referred to as KaY-1 and KaY-2, with a 12 Da increase in the mass (3443.38 Da) relative to sCT. The observation of two peaks of identical mass was expected, since there are two Lys residues in the sequence (Lys 11 and Lys18). Other minor side-products with crosslinks between Arg and Tyr and a mass of 3456.12 Da were also observed.[44] After semi-prep purification, we isolated 1 mg of KaY-1 and 5 mg of KaY-2. Although their retention times were different, these two analogues had identical mass and further study needed to be carried out to determine which Lys was crosslinked in each.

To perform a selective methylene crosslinking, and to identify which of the two Lys residues is bound to Tyr22 in each of these isomers, we decided to use the orthogonal PG trifluoroacetyl (Tfa), which is stable under acidic conditions. As such, the synthesis of sCT(Lys18-Tfa) was performed. After cleavage, oxidative folding and purification, the crosslinking with formaldehyde between the free Lys11 and Tyr22 was carried out on 30 mg sCT(Lys18-Tfa) at 37 °C overnight (Fig. S11, and ESI† for details). After purification by HPLC, the Tfa was removed in phosphate buffer at pH 13.[46] The peptide was purified again with semi-prep HPLC to give 5 mg of KaY-1 exclusively (16% yield) (confirmed by the retention time with the peak 1 from previous synthesis with sCT and their similar CD spectra, Fig. S13, ESI†). These results together with CD indicated that KaY-2 (which was isolated in sufficient amounts for the downstream characterizations, see below) has a methylene crosslink between Lys18 and Tyr22.

Using rational design, we suggested a single amino acid substitution to improve sCT's stability to enzymatic degradation. sCT has an Arg residue at position 24, which we found to

be one of the main cleavage sites by pancreatin enzymes,[47] so we decided to prepare a new analogue of KaY-1 in which Arg24 was replaced by glutamine, *i.e.*, KaY-1(R24Q). Indeed, hCT has a Gln at position 24, so the resulting CT mutant may be considered a hybrid of these two species (Fig. 1A, C and F and Scheme S1, ESI†).[42] For the preparation of KaY-1(R24Q), we first prepared CT(R24Q) with the Tfa PG on Lys18, and the same crosslinking reaction was performed (Fig. 1F and Fig. S14, ESI†) followed by the removal of the Tfa group and purification, which provided 2 mg of KaY-1(R24Q) (10% yield).

Next, the stability of sCT and its analogues was evaluated by their degradation in simulated gastric fluid (SGF) and simulated intestinal fluid (SIF) at 37 °C (Fig. 2B and C). The SGF contained pepsin at pH 1.3, while the SIF contained pancreatin at pH 6.8.[13] In the SGF the sCT had a half-life of only 35 min, whereas KaY-1 and KaY-1(R24Q) had a half-life of 190 and 170 min, respectively, while the other analogues did not exhibit any improvement in terms of stability (Table 1). Based on these encouraging results for KaY-1 and KaY-1(R24Q), we decided to test their stability in SIF. Gratifyingly, KaY-1(R24Q) was found to have a $t_{1/2}$ of 42 min, while sCT and KaY-1 had a $t_{1/2}$ of 5 and 7 min, respectively.

The calcitonin receptor (CTR) is a member of the G-protein-coupled receptors superfamily.[48] The activated receptor is capable of coupling to at least two signal transduction pathways, one of which leads to an increase in intracellular cAMP,[49] while the other is the phospholipase C pathway (PLC) which leads to the release of Ca^{2+} from intracellular stores and promotes the influx of external calcium.[50] Therefore, the *in vitro* activity of four of the most promising stabilized analogues with retained helical structures in addition to synthetic sCT, namely MT-CT, Se-CT, KaY-1 and KaY-1(R24Q), were tested. The ability of these analogues (in the range of 10 μM–1 pM) to activate the CTR, and as a result leading to an increase in the cytosolic cAMP and Ca^{2+} concentration (Fig. 2D and E), was evaluated.

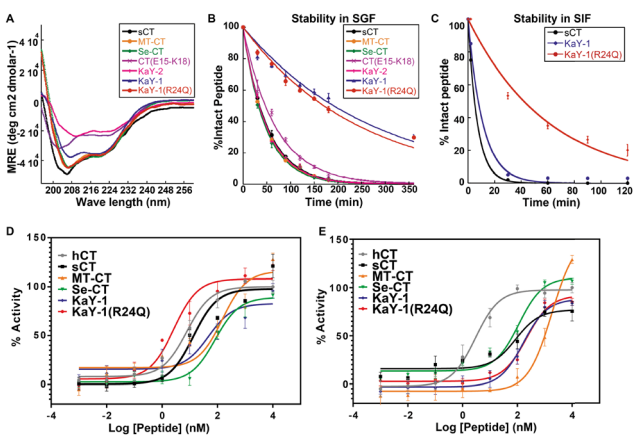

Fig. 2 CD spectra for CT analogues, the *in vitro* gastrointestinal stability and calcitonin receptor agonist assay for hCT, sCT, and analogues. (**A**) CD spectra for sCT and all analogues. (**B**) Stability in simulated gastric fluid (SGF). (**C**) Stability in simulated intestinal fluid (SIF). (**D**) cAMP accumulation assay using a Nomad biosensor. (**E**) Ca^{2+} assay using the HEK 293 CALCR-HiTSeeker cell line and the commercially available calcium assay kit. The data points were fitted to a first order decay function using Kaleidagraph to estimate the rate constants, which were used to calculate $t_{1/2}$, and all data were collected in triplicate. For activity, all data points represent mean ± SD for each condition and n = 3. (hCT is in gray, sCT in black, MT-CT in orange, Se-CT in green, CT(E_{15}-K_{18}) in purple, KaY-2 in pink, KaY-1 in blue, and KaY-1(R24Q) in red).

Table 1 Summary of the $t_{1/2}$ in SGF and SIF, and EC_{50} for cAMP and Ca^{2+} cytosolic concentration changes of CT analogues

CT analogue	SGF $t_{1/2}$ (min)	SIF $t_{1/2}$ (min)	cAMP EC_{50} (nM)	Ca^{2+} EC_{50} (nM)
hCT	n.d.	n.d.	7.8 ± 1.6	2.9 ± 0.6
sCT	35.6 ± 0.1	4.9 ± 0.7	13.5 ± 4.5	87.0 ± 17.5
MT-CT	33.5 ± 0.2	n.d.	1666 ± 60	7304 ± 700
Se-CT	32.6 ± 0.5	n.d.	82.7 ± 16.5	112.5 ± 18.3
CT(E_{15}–K_{18})	47.3 ± 1.9	n.d.	n.d.	n.d.
KaY-2	34.5 ± 0.3	n.d.	n.d.	n.d.
KaY-1	191.2 ± 66.1	7.1 ± 0.7	47.6 ± 24.1	165.5 ± 34.8
KaY-1(R24Q)	170.6 ± 32.2	41.9 ± 6.1	2.7 ± 0.8	215.8 ± 43.8

Innoprot's red $_{cAMP}$Nomad-CALCR U2OS cell line (a human bone osteosarcoma cell line) was used for cAMP accumulation assay (Fig. 2D and ESI† for details).[51] While the EC_{50} of hCT was determined at 7.78 nM, the sCT, Se-CT, KaY-1, and KaY-1(R24Q) also exhibit EC_{50} in the nanomolar range (Table 1), with KaY-1(R24Q) exhibiting a slightly enhanced potency (EC_{50} of 2.67 nM) compared to hCT, while MT-CT had EC_{50} > 1 μM.

The change in Ca^{2+} concentration was also measured using the HEK293 CALCR-HiTSeeker cell line and a commercially available calcium assay kit.[52] hCT showed a high efficacy (EC_{50} = 2.94 nM) compared with the synthetic analogues; 86.9 nM for sCT, 112 nM for Se-CT, 165 nM for KaY-1, and 215 nM for KaY-1(R24Q), while MT-CT had EC_{50} > 1 μM (Fig. 2E, Table 1).

In this study we aimed to produce other types of sCT analogues that would exhibit a higher resistance under simulated gastrointestinal conditions by taking advantage of peptide stapling. Therefore, we stabilized the disulfide bond by inserting methylene thioacetal (MT-CT) or a diselenide bridge (Se-CT). Furthermore, we applied the *i*, *i* + 3 lactam stapling approach to generate a crosslink between Glu15 and Lys18. In addition, we used cooperative stapling between a Lys and Tyr with formaldehyde to generate the *i*, *i* + 4 stapling product (KaY-2) and *i*, *i* + 11 stapling product (KaY-1). Finally, we replaced the arginine residue, which is a cleavage site for intestinal pancreatin peptidase, with glutamine to obtain KaY-1(R24Q).

CD characterization demonstrated that all but the CT(E_{15}–K_{18}) and KaY-2 analogues maintained their highly helical structure required for activity (Fig. 2A and ESI† for details).

The stability of sCT and its synthetic variants in the presence of pepsin and pancreatin was determined by following their overall rate of degradation. The results indicated that the two analogues KaY-1 and KaY-1(R24Q) have five-fold longer half-lives compared with the sCT and KaY-1(R24Q) exhibited an 8-fold increased stability in SIF compared to a much faster degradation of sCT and KaY-1 (Table 1). These findings support the proposed mechanism for CT degradation by pancreatin at Arg, and show that by eliminating this digestion site, the drug's efficacy may be increased.

The *in vitro* biological activity of the most stable synthetic analogues indicated that KaY-1(R24Q) displayed 3-fold more

activity than hCT in changing the cytosolic cAMP concentration. However, it was 70-fold less active than hCT in changing the calcium concentration in the cytosol. While KaY-1 showed 6-fold less activity in the cAMP assay, and 56-fold less activity in changing calcium concentrations in the cytosol in comparison to hCT.

In conclusion, the present study demonstrated that KaY-1(R24Q) obtained by stapling reaction between Lys11 and Tyr22 retained the helical structure, exhibited increased stability in both SGF and SIF, and retained activity. Our results provided a starting point for the development of an oral sCT analogue for the treatment of postmenopausal osteoporosis, Paget's disease and hypercalcemia.

N. M. acknowledges the financial support of the Israel Science Foundation (1388/22). H.G. thanks the British Council for GROWTH PhD Fellowship. We would like to thank Ms Ricki Notis Dardashti and Dr. Shay Laps for input on the manuscript.

Conflicts of interest

A provisional patent application covering this work has recently been filed.

Notes and references

1 D. Copp, *Annu. Rev. Physiol.*, 1970, **32**, 61–86.
2 J.-Y. Reginster, *Am. J. Med.*, 1993, **95**, S44–S47.
3 M. Azria, D. Copp and J. Zanelli, *Calcif. Tissue Int.*, 1995, **57**, 405–408.
4 G. Andreotti, B. L. Méndez, P. Amodeo, M. A. C. Morelli, H. Nakamuta and A. Motta, *J. Biol. Chem.*, 2006, **281**, 24193–24203.
5 E. Johansson, J. L. Hansen, A. M. K. Hansen, A. C. Shaw, P. Becker, L. Schaffer and S. Reedtz-Runge, *J. Biol. Chem.*, 2016, **291**, 13689–13698.
6 J. T. Potts Jr, *Bone Miner.*, 1992, **16**, 169–173.
7 M. Reches, Y. Porat and E. Gazit, *J. Biol. Chem.*, 2002, **277**, 35475–35480.
8 C. H. Chesnut III, S. Silverman, K. Andriano, H. Genant, A. Gimona, S. Harris, D. Kiel, M. LeBoff, M. Maricic and P. Miller, *Am. J. Med.*, 2000, **109**, 267–276.
9 S. J. Wimalawansa, *Calcif. Tissue Int.*, 1993, **52**, 90–93.
10 C. Wüster, W. Schurr, S. Scharla, F. Raue, H. Minne and R. Ziegler, *Eur. J. Clin. Pharm.*, 1991, **41**, 211–215.
11 A. Srinivasan, F. K. Wong and D. Karponis, *J. Musculoskeletal Neuronal Interact.*, 2020, **20**, 600.
12 J. H. Hamman, G. M. Enslin and A. F. Kotzé, *BioDrugs*, 2005, **19**, 165–177.
13 J. Wang, V. Yadav, A. L. Smart, S. Tajiri and A. W. Basit, *Mol. Pharmacol.*, 2015, **12**, 966–973.
14 M. Karsdal, I. Byrjalsen, K. Henriksen, B. Riis, E. Lau, M. Arnold and C. Christiansen, *Osteoarthritis Cartilage*, 2010, **18**, 150–159.
15 M. Karsdal, I. Byrjalsen, P. Alexandersen, A. Bihlet, J. Andersen, B. Riis, A. Bay-Jensen and C. Christiansen, *Osteoarthritis Cartilage*, 2015, **23**, 532–543.
16 G. L. Verdine and L. D. Walensky, *Clin. Cancer Res.*, 2007, **13**, 7264–7270.
17 J. E. Bock, J. Gavenonis and J. A. Kritzer, *ACS Chem. Biol.*, 2013, **8**, 488–499.
18 C. E. Schafmeister, J. Po and G. L. Verdine, *J. Am. Chem. Soc.*, 2000, **122**, 5891–5892.
19 Y. H. Lau, P. De Andrade, S.-T. Quah, M. Rossmann, L. Laraia, N. Sköld, T. J. Sum, P. J. Rowling, T. L. Joseph and C. Verma, *Chem. Sci.*, 2014, **5**, 1804–1809.
20 L. D. Walensky and G. H. Bird, *J. Med. Chem.*, 2014, **57**, 6275–6288.
21 J. Charoenpattarapreeda, Y. S. Tan, J. Iegre, S. J. Walsh, E. Fowler, R. S. Eapen, Y. Wu, H. F. Sore, C. S. Verma and L. Itzhaki, *Chem. Commun.*, 2019, **55**, 7914–7917.
22 P. M. Cromm, J. Spiegel and T. N. Grossmann, *ACS Chem. Biol.*, 2015, **10**, 1362–1375.
23 J. C. Phelan, N. J. Skelton, A. C. Braisted and R. S. McDowell, *J. Am. Chem. Soc.*, 1997, **119**, 455–460.
24 X. Li, S. Chen, W. D. Zhang and H. G. Hu, *Chem. Rev.*, 2020, **120**, 10079–10144.
25 R. Zhao, P. Shi, J. Y. Chen, S. S. Sun, J. N. Chen, J. B. Cui, F. M. Wu, G. M. Fang, C. L. Tian, J. Shi, D. Bierer, L. Liu and Y. M. Li, *Chem. Sci.*, 2020, **11**, 7927–7932.
26 H. X. Luong, H. T. P. Bui and T. T. Tung, *J. Med. Chem.*, 2022, **65**, 3026–3045.
27 R. B. Merrifield, *J. Am. Chem. Soc.*, 1963, **85**, 2149–2154.
28 W. J. Lees, *Curr. Opin. Chem. Biol.*, 2008, **12**, 740–745.
29 N. Metanis and D. Hilvert, *Angew. Chem., Int. Ed.*, 2012, **51**, 5585–5588.
30 C. Kourra and N. Cramer, *Chem. Sci.*, 2016, **7**, 7007–7012.
31 R. Mousa, S. Lansky, G. Shoham and N. Metanis, *Chem. Sci.*, 2018, **9**, 4814–4820.
32 O. Weil-Ktorza, N. Rege, S. Lansky, D. E. Shalev, G. Shoham, M. A. Weiss and N. Metanis, *Chem. – Eur. J.*, 2019, **25**, 8513–8521.
33 M. Muttenthaler, Å. Andersson, I. Vetter, R. Menon, M. Busnelli, L. Ragnarsson, C. Bergmayr, S. Arrowsmith, J. R. Deuis and H. S. Chiu, *Sci. Sign.*, 2017, **10**, eaan3398.
34 R. Mousa, T. Hidmi, S. Pomyalov, S. Lansky, L. Khouri, D. E. Shalev, G. Shoham and N. Metanis, *Commun. Chem.*, 2021, **4**, 1.
35 M. Muttenthaler, A. Andersson, A. D. de Araujo, Z. Dekan, R. J. Lewis and P. F. Alewood, *J. Med. Chem.*, 2010, **53**, 8585–8596.
36 J. Bondebjerg, M. Grunnet, T. Jespersen and M. Meldal, *ChemBioChem*, 2003, **4**, 186–194.
37 A. M. Spokoyny, Y. Zou, J. J. Ling, H. Yu, Y. S. Lin and B. L. Pentelute, *J. Am. Chem. Soc.*, 2013, **135**, 5946–5949.
38 Y. Zheng, L. Zhai, Y. Zhao and C. Wu, *J. Am. Chem. Soc.*, 2015, **137**, 15094–15097.
39 Y. K. Qi, Q. Qu, D. Bierer and L. Liu, *Chem. – Asian J.*, 2020, **15**, 2793.
40 M. J. Klein, S. Schmidt, P. Wadhwani, J. Bürck, J. Reichert, S. Afonin, M. Berditsch, T. Schober, R. Brock and M. Kansy, *J. Med. Chem.*, 2017, **60**, 8071–8082.
41 J. W. Taylor, *Pep. Sci.*, 2002, **66**, 49–75.
42 J. W. Taylor, Q. K. Jin, M. Sbacchi, L. Wang, P. Belfiore, M. Garnier, A. Kazantzis, A. Kapurniotu, P. F. Zaratin and M. A. Scheideler, *J. Med. Chem.*, 2002, **45**, 1108–1121.
43 R. Beugelmans, L. Neuville, M. Bois-Choussy, J. Chastanet and J. Zhu, *Tetrahedron Lett.*, 1995, **36**, 3129–3132.
44 B. Li, H. Tang, A. Turlik, Z. Wan, X. S. Xue, L. Li, X. Yang, J. Li, G. He, K. N. Houk and G. Chen, *Angew. Chem., Int. Ed.*, 2021, **60**, 6646–6652.
45 B. Li, L. Wang, X. Chen, X. Chu, H. Tang, J. Zhang, G. He, L. Li and G. Chen, *Nat. Commun.*, 2022, **13**, 1–9.
46 S. Bartoli, K. B. Jensen and J. D. Kilburn, *J. Org. Chem.*, 2003, **68**, 9416–9422.
47 D. C. Whitcomb, M. C. Gorry, R. A. Preston, W. Furey, M. J. Sossenheimer, C. D. Ulrich, S. P. Martin, L. K. Gates Jr, S. T. Amann and P. P. Toskes, *Nat. Genet.*, 1996, **14**, 141–145.
48 L. Masi and M. L. Brandi, *Clin. Rev. Bone Miner. Metab.*, 2007, **4**, 117.
49 N. Hunt, M. Ellison, J. Underwood and T. Martin, *Br. J. Cancer*, 1977, **35**, 777–784.
50 M. Pondel, *Int. J. Exp. Pathol.*, 2000, **81**, 405–422.
51 R. M. Mella, D. Kortazar, M. Roura-Ferrer, C. Salado, M. Valcárcel, A. Castilla and P. Villacé, *SLAS Technol.*, 2018, **23**, 207.
52 K. R. Gee, K. Brown, W. U. Chen, J. Bishop-Stewart, D. Gray and I. Johnson, *Cell Calcium*, 2000, **27**, 97–106.